JGR Earth Surface

RESEARCH ARTICLE
10.1029/2018JF004758

Elucidating Coastal Foredune Ecomorphodynamics in the U.S. Pacific Northwest via Bayesian Networks

R. G. Biel[1], **S. D. Hacker**[1], **and P. Ruggiero**[2]

[1]Department of Integrative Biology, Oregon State University, Corvallis, OR, USA, [2]College of Earth, Ocean, and Atmospheric Sciences, Oregon State University, Corvallis, OR, USA

Key Points:

- Sediment supply and beach type influence both foredune morphology and rates of foredune change
- Foredune morphology and rates of foredune change are influenced by species-specific beachgrass density and growth form patterns
- Foredune ecomorphodynamics differ among the beachgrass congeners, *Ammophila arenaria* and *Ammophila breviligulata*

Supporting Information:

- Supporting Information S1
- Table S1
- Table S2
- Table S3
- Table S4
- Table S5

Correspondence to:
R. G. Biel,
reuben.biel@gmail.com

Citation:
Biel, R. G., Hacker, S. D., & Ruggiero, P. (2019). Elucidating coastal foredune ecomorphodynamics in the U.S. Pacific Northwest via Bayesian networks. *Journal of Geophysical Research: Earth Surface*, *124*, 1919–1938. https://doi.org/10.1029/2018JF004758

Received 15 MAY 2018
Accepted 20 MAY 2019
Accepted article online 5 JUL 2019
Published online 23 JUL 2019

Abstract As sea level rise and possible changes in storminess threaten coastal communities and infrastructure, the capacity for foredunes to provide protection depends on their geomorphology, which is determined by interactions between physical beach processes and vegetation. Here we use descriptive Bayesian network analyses to examine how sediment supply, beach characteristics, and two species of beachgrass (*Ammophila arenaria* and *Ammophila breviligulata*) alter foredune morphology and patterns of sand accretion on U.S. Pacific Northwest foredunes. We show that sediment supply and beach type primarily determine foredune morphology. Beachgrass density also influences foredune shape, but its effects differ among species: increasing density of *A. arenaria* was associated with steeper sloping dunes, whereas increasing density of *A. breviligulata* was associated with wider, more shallow sloping dunes. An examination of the change in foredune morphology over a 2-year period found sand accretion was most strongly influenced by species-specific patterns of vegetation growth and beach type. Specifically, *A. breviligulata* exhibited more lateral growth, resulting in greater sand accretion at the seaward margin of the foredune. In contrast, *A. arenaria* exhibited little lateral growth, resulting in comparatively more sand accretion near the foredune crest. Consequently, growth form-generated sand accretion patterns resulted in steep, narrow *A. arenaria*-dominated foredunes and shallow-sloping, wider *A. breviligulata*-dominated foredunes. These results illustrate that vegetation density and patterns of growth influence foredune morphology and its changes over time.

1. Introduction

Sandy beaches and dunes represent one of the most important ecosystems for regulating coastal hazard exposure and also provide many cobeneficial ecosystem services (Barbier et al., 2011; Everard et al., 2010). As increasing coastal development, extreme storms, and sea level rise have caused unprecedented and growing property damage in recent decades (Intergovernmental Panel on Climate Change, 2014; Pielke et al., 2008), coastal foredunes are increasingly promoted as a natural infrastructure solution for mitigating damage (Bloomberg, 2013; Hanley et al., 2014; Spalding et al., 2014). Foredunes impede wave overwash and inundation during storms by providing a barrier to wave attack and by supplying sediment, via dune erosion, to beaches during storms (Kriebel & Dean, 1985; Morton, 2002). Yet the severity of flooding and erosion during storm events depends not only on the duration and intensity of wave impacts (Larson et al., 2004) but also on beach slope, foredune width, and foredune height (Morton, 2002; Plant & Stockdon, 2012; Sallenger, 2000). Thus, the capacity for dunes to provide coastal protection depends, in part, on their prestorm geometry (Hatzikyriakou et al., 2015; Stockdon et al., 2007). However, effective utilization of foredunes for coastal protection will require a greater understanding about the degree to which they provide protection, their spatiotemporal variation in protection, and their recovery and long-term resilience following storms (Sutton-Grier et al., 2015).

Coastal foredunes are ecomorphodynamic systems in which geomorphology and landform dynamics influence (and are influenced by) ecological processes (Corenblit et al., 2011). Although dune vegetation is well recognized to alter and be altered by patterns of aeolian sediment deposition on foredunes and influence foredune formation and shape (Duran & Moore, 2013; Hacker et al., 2012; Hesp, 1989, 2002; Keijsers et al., 2015, 2016; Zarnetske et al., 2012, 2015), most geomorphological research focuses on sediment supply, sediment characteristics, and wind as determinants of foredune geomorphology. Based on empirical observations and conceptual models, dissipative beaches with wide fetches provide greater sand supplies to foredunes than narrow, reflective beaches, given a similar wind climate (Bauer et al., 2009; Bauer &

Davidson-Arnott, 2003; Walker et al., 2017). Because beach slope results from interactions between sediment grain size distributions and the wave climate, dissipative beaches are typically characterized by fine-grained sediments and persistently high wave energy (Wright & Short, 1984). Consequently, this combination of fine grain sizes and wide fetches on dissipative beach types may promote the formation of large foredunes through heightened aeolian sand transport (Houser et al., 2008; Houser & Mathew, 2011; Saye et al., 2005; Short & Hesp, 1982).

Beach-dune sediment budgets (i.e., the net sediment surplus or deficit on beaches and on dunes per unit area and time) and rates of shoreline change may also alter foredune morphology. Progradation (seaward expansion of the shoreline) results from positive beach sediment budgets and often produces dune fields composed of multiple active and relict dunes. However, due to the rapid rate of dune ridge formation, prograding shorelines are associated with short foredunes, despite positive dune sediment budgets. In contrast, neutral or slightly retreating shorelines with neutral or slightly negative beach sediment budgets are associated with taller foredunes (Moore et al., 2016; Psuty, 1988; Ruggiero et al., 2016).

Although beach morphology, wind regime, and sediment supply are considered the primary determinants of foredune shape, the influence of vegetation on foredune morphology remains relatively understudied. Vegetation density, height, and growth form are associated with different dune forms: low or patchy plant density often produces local variations in sediment deposition, leading to the formation of dunelets or hummocks. In contrast, dense, tall vegetation produces more uniform sediment deposition, leading to the formation of continuous, linear foredunes (Hesp, 1989, 2002). Based on models and small-scale experiments, increasing plant density and height cause increasing foredune height but decreasing width (Arens et al., 2001; Hesp, 1989; Van Dijk et al., 1999). While several studies examine the role of vegetation in foredune evolution using numerical models (Duran & Moore, 2013; Goldstein et al., 2017; Moore et al., 2016; Van Dijk et al., 1999) and wind tunnel experiments (Zarnetske et al., 2012), field studies that link vegetation patterns to foredune morphology are rare (Hacker et al., 2012; Hesp, 1983). Moreover, fewer examine the relative influence of geomorphological and ecological drivers on foredune morphology (e.g., Zarnetske et al., 2015).

To explore the relative roles of geomorphological drivers and vegetation species identity and morphology for influencing foredune geomorphology and evolution, we examined ecological and geomorphological spatiotemporal variability in U.S. Pacific Northwest coastal dunes. The Pacific Northwest exhibits varied beach types that range from highly dissipative to intermediate reflective (Mull & Ruggiero, 2014; Ruggiero et al., 2005). Shoreline change rates (SCRs) also vary because of spatial variation in beach sediment budgets, producing average multidecadal progradation rates in excess of 3 m/year in some littoral cells and average shoreline retreat of 0.5 m/year in others (Buijsman et al., 2003; Ruggiero et al., 2013). Consequently, the region exhibits substantial variations in geomorphological drivers of foredune morphology, including shoreface slope, beach slope, and beach sediment budgets.

Additionally, the Pacific Northwest dune system is dominated by two species of invasive beachgrasses, *Ammophila arenaria* (L.) Link and *Ammophila breviligulata* Fernald. Since their introduction in the early twentieth century, the two species have spread and monopolized foredunes along the entire Pacific coast and formed dense monocultures on the foredune face and crest (Hacker et al., 2012; Wiedemann & Pickart, 1996). *Ammophila arenaria* and *A. breviligulata* are implicated in producing unique dune morphotypes, such that *A. arenaria*-dominated foredunes are often taller and narrower than their *A. breviligulata*-dominated counterparts (Hacker et al., 2012; Zarnetske et al., 2012, 2015). These differences are hypothesized to occur because of species-specific differences in plant morphology and growth form. *Ammophila arenaria* has thin but dense stems (known as tillers) and form tussocks that efficiently capture sand. In contrast, *A. breviligulata* has more robust stems but they are more sparsely distributed and thus capture less sand per given area (Zarnetske et al., 2012). Nevertheless, spatially correlated geomorphological and ecological drivers of foredune morphology have confounded rigorous regression analyses of the relationship between beachgrass species identity and foredune morphology (Hacker et al., 2012).

Here we build on previous research (Zarnetske et al., 2015) by disentangling the relative effects of beach and dune geomorphology and beachgrasses using descriptive Bayesian networks (BNs; Beuzen et al., 2018). We explore two aspects of foredune ecomorphodynamics: first, we consider the relative contributions of sediment supply, shoreface and beach morphology, and vegetation species identity and density to foredune morphology; second, we consider how these same variables influence change in foredune morphology via rates of vertical sand accretion across the foredune face. We hypothesize that backshore slope (as a proxy for beach type), SCR (as a proxy for beach sediment budget), and beachgrass density relate to foredune height and rates of vertical sand accretion (H_1). If patterns described by Short and Hesp (1982) hold, then shallow-sloping beaches should be positively associated with both foredune height and rates of vertical accretion. Alternatively, SCR may disparately influence foredune morphology and sand accretion: while progradation may accelerate sand accretion because of positive beach and dune sediment budgets, it may also produce shorter foredunes through development of multiple dune ridges. Based on wind tunnel experiments, field experiments, and numerical models (Hesp, 1989; Van Dijk et al., 1999; Zarnetske et al., 2012), we further hypothesize that increasing beachgrass stem density will be associated with taller and narrower foredunes (H_2), that inclusion of species-specific stem density variables will improve the accuracy and precision of the BN for predicting foredune morphology (H_3), and that *A. breviligulata* stem density will be more positively associated with foredune height than *A. arenaria* stem density due to species-specific differences in stem morphology (H_4).

2. Methods and Analyses

2.1. Study Sites, Beach and Foredune Geomorphology, and Vegetation Surveys

To measure foredune geomorphology and vegetation abundance, we conducted dune surveys in the summers of 2012 and 2014 at 20 sites spanning 500 km along the Oregon and southwest Washington coastlines, United States (Figure 1a and Table S1 on the supporting information; Biel et al., 2019; Hacker et al., 2012). Sites are located within 11 distinct littoral or sublittoral cells (Inman & Frautschy, 1965) and differ in sand supply and beach and dune geomorphology (Mull & Ruggiero, 2014).

Among these 20 sites, we established 233 shore-normal transects at 80 transect locations (3 transects per location and 2–10 transect locations per site; see Figure 1b and Table S1) and conducted topographic surveys to determine the elevation between the waterline and foredune heel (d_h) using network real time kinematic differential GPS (Figure 1c; see methods in Biel et al., 2017; Ruggiero et al., 2005). Using methods by Mull and Ruggiero (2014), we then identified the position of the shoreline (defined as mean high water [MHW]) and the position and elevation of several metrics of foredune morphology (foredune defined as the seaward-most shore-parallel sand ridge, whose landward extent is delimited by a 0.6 m or greater elevation drop relative to the maximum elevation of the foredune, Cooper, 1958; Mull & Ruggiero, 2014). Foredune measurements included the position and elevation of the foredune toe (d_t = the seaward-extent of the foredune), the foredune crest (d_c), and foredune heel (d_h = landward extent of the seaward-most dune ridge, demarcated by an elevation minima; Figure 1c). From these metrics, we determined backshore slope (slope between MHW and d_t), foredune face slope (d_{face} slope; slope between d_t and d_c locations), and foredune width (horizontal distance between d_t and d_h locations) along each cross-shore transect. We also calculated shoreface slope (defined as the slope between 10 and 15 m below local mean sea level, LMSL) along each transect from National Oceanic and Atmospheric Administration tsunami inundation digital elevation model (DEM) data sets (Carignan et al., 2009; Carignan et al., 2009b, 2009a; Love et al., 2012). .

For each transect, we characterized sediment supply using a multidecadal rate of shoreline change (SCR), measured as an annualized rate of shoreline change between 1967 and 2002 in Oregon and 1986–2002 in southwest Washington (Ruggiero et al., 2013).

We also characterized dune vegetation density by conducting georeferenced vegetation surveys along each of the 233 transects in 2012. Along each transect, we measured the abundance of all plant species within 0.25-m^2 quadrats at 5-m intervals as described in Hacker et al. (2012) and Biel et al. (2017) and calculated mean beachgrass density (beachgrass tillers per m^2) per transect for both *Ammophila* species along the foredune face (between the 4 m contour and d_c). Finally, in 2014, we resurveyed topography and vegetation along 70 of the transects that were surveyed in 2012 (Table S1) and determined the changes in beachgrass density and elevation for each georeferenced quadrat location between 2012 and 2014. Of the 320 quadrat locations on the foredune face that were surveyed in both 2012 and 2014, 273 locations (85%) exhibited positive elevation change, indicating accretion of sand. Correspondingly, no major storm events occurred during this time period. Analyses were performed in ArcGIS v10.3.1, R v.3.4.3 (R Core Team, 2015), and Matlab R2015b.

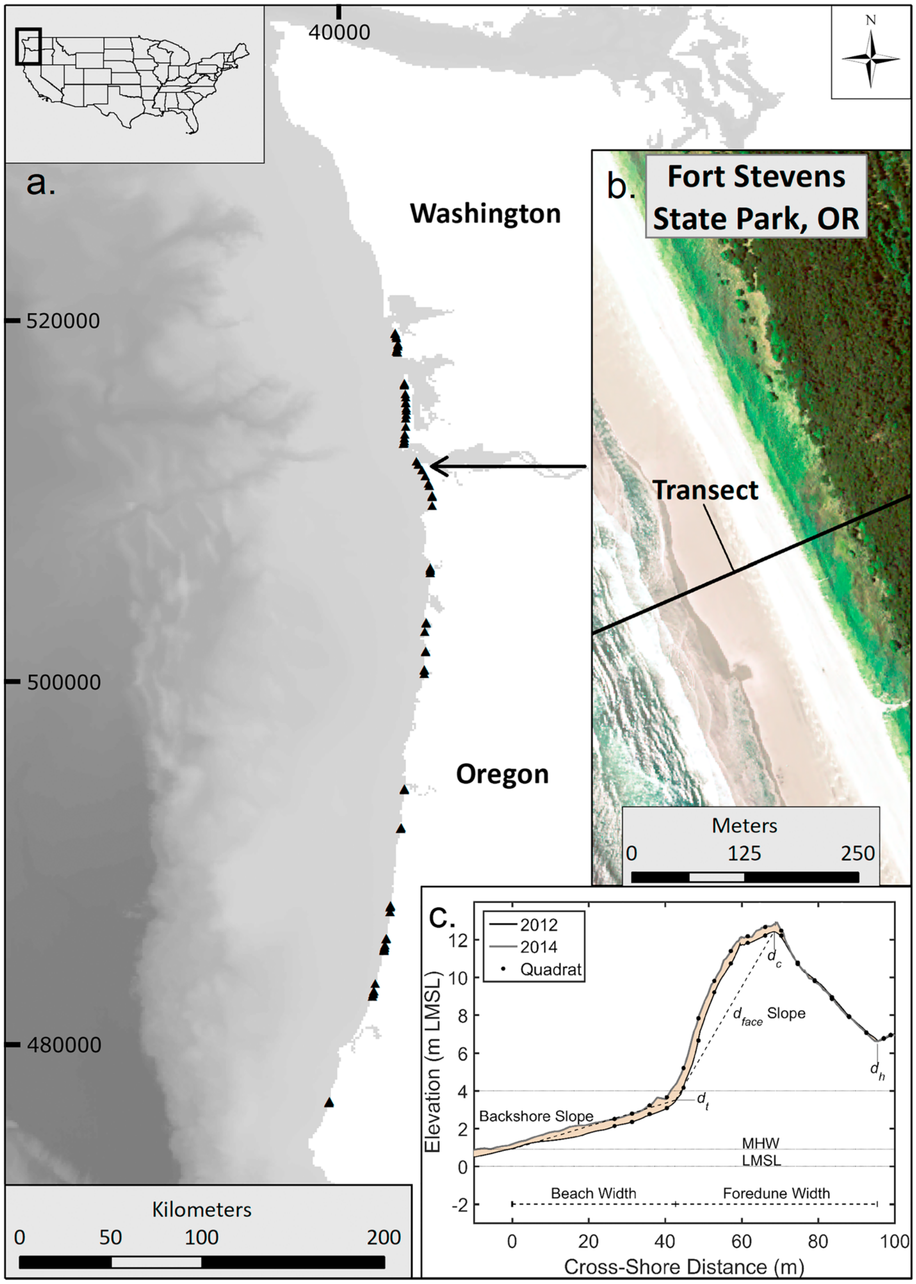

Figure 1. (a) Topographic and vegetation transect locations in Oregon and southwest Washington, United States (Table S1). Inset images illustrate (b) a cross-shore transect perpendicular to the foredune at Fort Stevens, OR (FS02), and (c) its corresponding smoothed cross-shore topographic profile and foredune morphometrics for 2012 and 2014. Tan polygon indicates sand accretion over 2 years. Black points indicate quadrat placement in 2012 (lower foredune profile; black) and 2014 (upper foredune profile; gray). The foredune crest (d_c) is the elevation maximum on the seaward-most foredune. The foredune toe (d_t) is the topographic inflection point between the backshore and the foredune. Backshore slope is the slope between the shoreline (at mean high water [MHW]) and d_t. Foredune face slope (d_{face} slope) is the slope between d_t and d_c. Foredune width is the horizontal distance between d_t and d_h. LMSL = local mean sea level.

2.2. Bayesian Network Analysis

We use BNs to explore how sediment supply, beach characteristics, and the two *Ammophila* species influence foredune morphology and patterns of sand accretion on foredunes, using data described in section 2.1. BNs are probabilistic graphical models that describe direct relationships among a network of variables using directed acyclic graphs (DAG; Koller et al., 2009; Needham et al., 2007). BNs are an

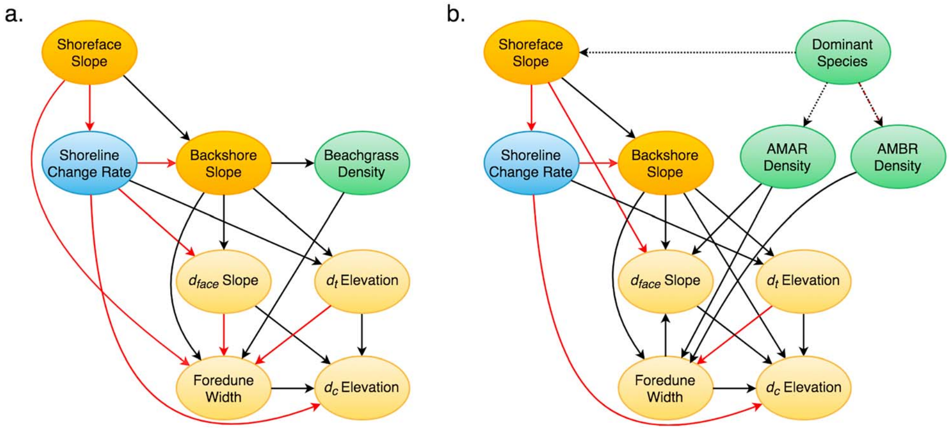

Figure 2. Gaussian Bayesian network and conditional linear Gaussian network graphical models illustrating direct and indirect relationships among the two *Ammophila* species, and shoreface, beach, and foredune morphometrics. Dotted lines indicate multinomial relationships; black lines indicate positive direct relationships and red lines indicate negative direct relationships. (a) GBN in which *A. arenaria* and *A. breviligulata* densities are pooled into a unified beachgrass density variable (Morphology-GBN$_{\text{combined}}$). (b) CLGN in which *A. arenaria* and *A. breviligulata* densities are treated as separate nodes (Morphology-CLGN$_{\text{species}}$). Variable definitions presented in Table S2. GBN = Gaussian Bayesian network; CLGN = Conditional Linear Gaussian network.

effective and flexible tool for examining coastal morphodynamics, as they can represent complex conditional relationships among variables and allow for input of prior system knowledge to test hypotheses and improve predictions (e.g., Beuzen et al., 2018; Gutierrez et al., 2011, 2015; Plant & Stockdon, 2012). BNs are characterized by both structure learning and parameter learning components. In the structure learning component, all independent, conditionally independent, and dependent relationships are identified within the multivariate system and depicted using a DAG. In a DAG (e.g., Figure 2), variables (nodes) are represented by ovals and direct dependent relationships between parent and child nodes are denoted by arrows (edges). Upon identifying the BN structure, the model is parameterized by calculating the joint probability distribution of the entire BN and conditional probability distributions for each node.

Multiple types of BNs exist, depending upon the type of data that they represent within their nodes. BNs may consist of discrete variables only (discrete BN), continuous variables only (e.g., Gaussian Bayesian network), or a combination of discrete and continuous variables (Hybrid Bayesian network). Discrete BNs are well represented within coastal geomorphology and engineering (e.g., Gutierrez et al., 2011; Plant et al., 2014; Plant & Stockdon, 2012; Poelhekke et al., 2016). Although discrete BNs are effective for modeling nonlinear systems and categorical data (Plant & Stockdon, 2012), discretization of continuous variables leads to information loss, may result in misclassification (e.g., Beuzen et al., 2018) and typically require large data sets for parameterization of conditional probability tables.

To avoid information loss and to leverage linear relationships among variables in our data set, we implemented Gaussian Bayesian networks (GBNs) and Conditional Linear Gaussian networks (CLGNs) to investigate connections between geomorphological drivers, ecological drivers, and foredune shape. GBNs assume that the joint probability distribution of all random variables ($\boldsymbol{X}$) is multivariate Gaussian, and that the conditional probability density function for each variable $Y \in \boldsymbol{X}$ with (continuous) parent variables ($\boldsymbol{X_C}$) is univariate Gaussian:

$$p(Y|\boldsymbol{X_C} = \boldsymbol{X_C}) = N\left(\beta_o + \beta^T \boldsymbol{X_C}, \sigma\right)$$

where β are coefficients of linear regression. Therefore, the conditional mean of Y is a linear model of its parent variables $\boldsymbol{X_c}$, with standard deviation σ.

CLGNs are a generalization of GBNs that contain both discrete (multinomial; $X_D \in \boldsymbol{X}$) and continuous (Gaussian; $X_C \in \boldsymbol{X}$) variables and are a special case of a hybrid Bayesian network (Salmerón et al., 2015). In CLGNs, discrete-discrete, discrete-Gaussian, and Gaussian-Gaussian parent-child hierarchies are permitted, but Gaussian-discrete parent-child hierarchies are prohibited. Correspondingly, the conditional distribution of discrete variables given discrete parents $p(Y_D|\boldsymbol{X_D} = \boldsymbol{X_D})$ is multinomial; the conditional distribution of Gaussian variables given Gaussian parents $p(Y_C|\boldsymbol{X_C} = \boldsymbol{X_C},)$ is Gaussian; and the conditional distribution of Gaussian variables given discrete (or discrete and continuous) parents is

$$\mathrm{p}(\mathrm{Y_C}|\mathbf{X_C} = \mathbf{X_C}, \mathbf{X_D} = \mathbf{X_{D_i}}) = \mathrm{N}\left(\beta_o(\mathrm{X_{D_i}}) + \beta^{\mathrm{T}}(\mathrm{X_{D_i}})\mathbf{X_c}, \sigma(\mathrm{X_{D_i}})\right)$$

such that the β and σ vary by D_i and form a mixture of Gaussians across all categories of $\boldsymbol{X_D}$ (Ramos-López et al., 2018).

2.2.1. Models of Foredune Morphology

To assess how shoreface morphology, beach morphology, and beachgrass density relate to foredune morphology (H_1-H_2), we created a GBN (named Foredune Morphology-GBN$_{\mathrm{combined}}$) to relate SCR, shoreface slope, backshore slope, and vegetation (mean beachgrass density on d_{face}) to foredune morphometrics (d_t elevation, d_c elevation, d_{face} slope, and foredune width; Figure 2a). Although the age of dunes likely also contributes to foredune morphology, a lack of historical data for most locations precludes the determination of their age. To further examine whether the two species of beachgrass were associated with distinct foredune morphologies (H_3-H_4), we created a CLGN (named Foredune Morphology-CLGN$_{\mathrm{species}}$) that separated mean beachgrass density into its component species, *A. arenaria* and *A. breviligulata*, and defined a parent categorical variable to classify the dominant species along each transect (Figure 2b). To meet Gaussian distributional assumptions, variables were transformed using log and box-cox transformations, as necessary (Table S2).

To identify direct relationships among variables (i.e., structure learning), we used both user knowledge and machine learning to identify an optimal network structure. User knowledge was incorporated into the BNs by prohibiting (blacklisting) or including (whitelisting) direct relationships (edges) between variables that we considered unlikely or likely, given our understanding of the system (Table S3). For processes where relationships are bidirectional or cyclic (e.g., feedback cycles; Duran & Moore, 2013), we selected relationship directionality based on the hypothesized dominant interaction. For example, we hypothesized that SCR was directly related to d_c elevation. This direct association could be represented within the BNs as (SCR ➔ d_c elevation) or as (d_c elevation ➔ SCR). Given our understanding of the dominant cause-effect relationship between SCR and d_c elevation in the Pacific Northwest (based on Psuty, 2008; Moore et al., 2016), we prohibited (d_c elevation ➔ SCR) as a possible direct relationship.

We further employed a hill-climbing algorithm to identify the best supported DAG structure, given the observed data set. We generated 100 random initial DAGs and implemented the hill-climbing algorithm, which iteratively added, removed, or reversed edges (excluding blacklisted edges) within each DAG. With each iteration, we then used a (conditional) Gaussian Akaike Information Criterion score (AIC-g, AIC-cg; Akaike, 1974) to assess whether these changes increased the likelihood of the BN's posterior distribution, given the observed data set. Iterative modification of edges allowed for identification of 100 BNs with local AIC-g (AIC-cg) score minima. Moreover, use of AIC-based scoring further limited model complexity by penalizing the network likelihood score with parameterization of each additional edge, thereby reducing overfitting. To identify the globally optimal BN, we performed model averaging to compute the average network structure (Scutari & Denis, 2014). We note that spatial autocorrelation exists in this data set because of the nested sampling design. Although modeling of dependent relationships in these BNs reduces autocorrelation in the residuals, it does not completely eliminate it. Even so, few BNs can directly correct for spatial autocorrelation (Trifonova et al., 2015), and they are commonly overlooked in spatial BN applications (Gutierrez et al., 2015; Plant & Stockdon, 2012). BN modeling was performed using bnlearn (Scutari & Denis, 2014) and rbmn (Denis, 2013) in R v3.22 (R Core Team, 2015).

2.2.2. Models of Change in Foredune Morphology

Although the foredune morphology BNs demonstrate how sediment supply, beach morphology, and beachgrass densities relate to foredune morphology, they cannot capture how beachgrass growth form and spatial distributions may influence foredune development. To more precisely explore how the distribution, density, and growth form of beachgrasses, as well as beach sediment supply, and shoreface and beach morphology influence foredune morphology along d_{face}, we implemented two additional CLGNs to relate spatiotemporal changes in beachgrass density to changes in elevation along d_{face} quadrats over time. Using data from 320 quadrats located along the d_{face} of 70 transects that were sampled in both 2012 and 2014, we identified

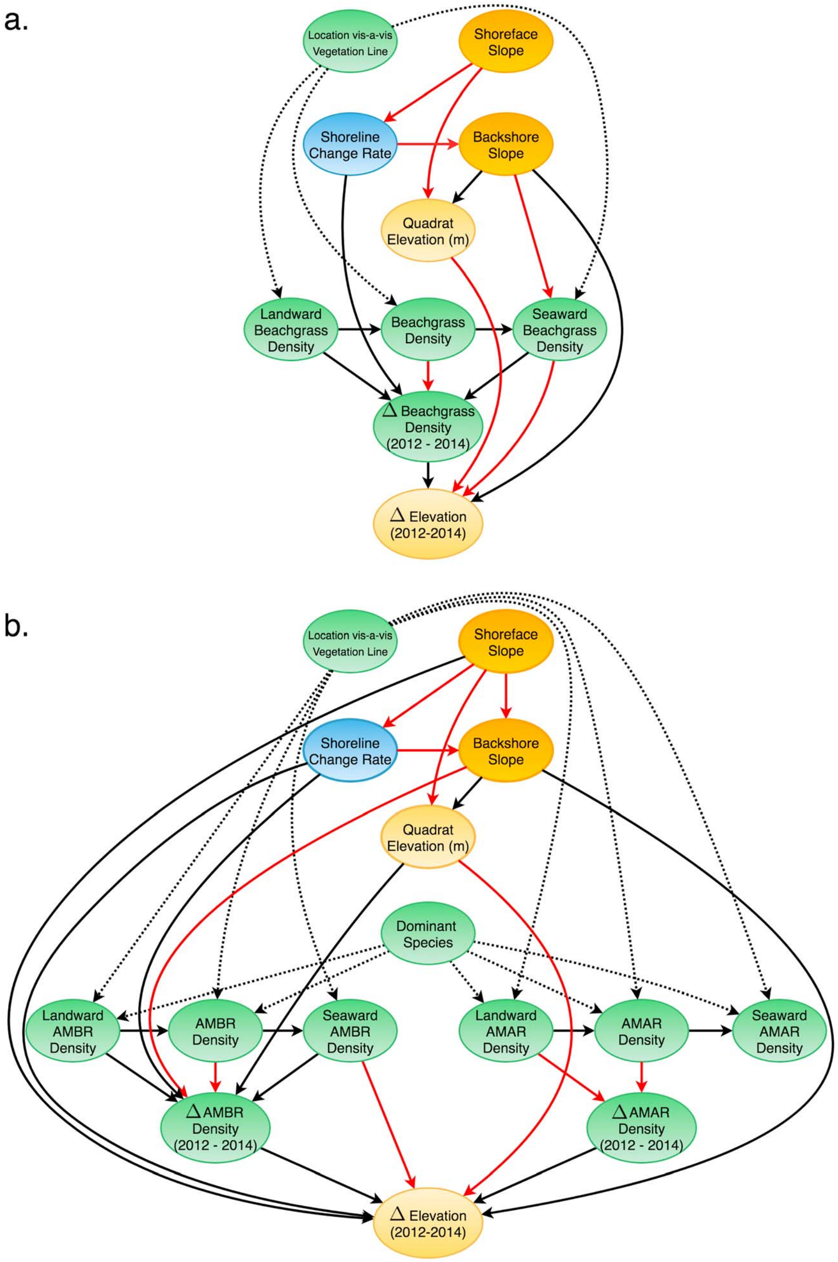

Figure 3. Conditional linear Gaussian network (CLGN) graphical models illustrating direct and indirect relationships among *Ammophila* density, shoreface and beach morphometrics, and sand accretion rates at quadrats along the foredune face between 2012 and 2014. Beachgrass density is that from 2012. Landward and seaward beachgrass density indicates beachgrass density in quadrats directly landward and seaward of the sampled quadrat in 2012. Δ beachgrass density (2012–2014) is the log response ratio of beachgrass density in the sampled quadrat between 2012 and 2014. Dotted lines indicate multinomial relationships; black lines indicate positive direct relationships and red lines indicate negative direct relationships. (a) CLGN in which *Ammophila arenaria* and *A. breviligulata* densities are pooled into unified beachgrass density variables (Accretion-CLGN$_{\text{combined}}$). (b) CLGN in which *A. arenaria* (AMAR) and *A. breviligulata* (AMBR) densities are treated as separate nodes (Accretion-CLGN$_{\text{species}}$). Variable definitions presented in Table S4.

relationships between measures of beach sediment supply, beach morphology, vegetation density and growth patterns, and changes in elevation (H_1-H_2). The modeled variables were SCR, shoreface slope, beach slope, quadrat elevation in 2012, quadrat log (beachgrass density) in 2012, log (beachgrass density) in directly adjacent quadrats (5 m landward and seaward), and changes in both log (beachgrass density) and foredune elevation between 2012 and 2014 (Accretion-CLGN$_{\text{combined}}$; Figure 3a and Table S4). We included a categorical variable to indicate whether the quadrat occurred landward or seaward of the seaward-most occurring *Ammophila* along each transect.

To further examine possible impacts of beachgrass species identity (H_3-H_4), we separated all beachgrass variables into their respective species and defined a categorical parent variable to identify the dominant species within the transect (Accretion-CLGN$_{\text{species}}$; Figure 3b). For both the Accretion-CLGN$_{\text{combined}}$ and Accretion-CLGN$_{\text{species}}$ networks, we prohibited and required specific edges (Tables S5 and S6) based on user knowledge (and to meet CLGN statistical assumptions), generated 100 random initial DAGs, and implemented a hill climbingalgorithm to identify locally optimal network structures. Model averaging was then performed to identify the globally optimal network structure for the two foredune change CLGNs. Upon identification of the optimal CLGN structures, we parameterized relationships between nodes using each respective data set.

2.3. Bayesian Network Performance Evaluation

BNs use a Bayesian approach for predicting outcomes and their associated uncertainty, based on Bayes theorem:

$$\text{Posterior distribution} \propto \text{Likelihood} \times \text{Prior distribution}$$

where the likelihood associated with each BN node is the relative likelihood of observing any condition in the sample space; the prior distribution represents one's knowledge or belief about the sample space, and the posterior is the probability density function for observing a condition in the sample space, after accounting for prior system knowledge. Based on this framework, BNs allow input of user knowledge through two avenues: first, through the specification of network structure as previously described; and second, by combining known information about a system (via constraints on the priors) with empirical data (likelihood function) to predict both the expected outcome and uncertainty associated with a target node (posterior distribution). This process of updating the posterior distribution based on prior knowledge is useful for prediction, for evaluation of model performance, and for evaluation of the relative importance of nodes within a model.

To assess the descriptive skills of each GBN and CLGN, we determined the log-likelihood ratio (LLR), root-mean-square error (RMSE), and Efron's pseudo R^2 between observed and predicted values of target nodes, based on different combinations of updated (prior) knowledge. LLR, RMSE, and pseudo R^2 values were determined by comparing BN predictions of foredune geomorphology target variables (e.g., d_c elevation, d_t elevation, d_{face} width, and d_{face} slope) with observed data and are both measures of BN descriptive accuracy and precision. The log-likelihood ratio was calculated as the log ratio of the likelihood of observations under a posterior distribution relative to the likelihood of observations under a prior distribution,

$$\text{LLR} = \sum_{i=1}^{N} \log\left(\frac{L\left(\text{obs}_i \sim N\left(\mu_i^{\text{post}}, v_i^{\text{post}}\right)\right)}{L\left(\text{obs}_i \sim N\left(\mu_i^{\text{prior}}, v_i^{\text{prior}}\right)\right)}\right)$$

where the prior and posterior distributions for the target node were determined by inclusion or exclusion of updated knowledge, respectively (Gutierrez et al., 2011). Correspondingly, Log (Bayes factor) is the Bayesian equivalent of LLR (Kass & Raftery, 1995). Here, we compared (1) the likelihood of observed data under a BN model with one known predictor only to a null model ($\text{LLR} = \log\left[L(\text{data} \mid \text{BN}_{\text{Null}+1})/L(\text{data} \mid \text{BN}_{\text{Null}})\right]$) and (2) the likelihood of observed data under a BN model with full knowledge to that with knowledge of all but one predictor ($\text{LLR} = \log\left[L(\text{data} \mid \text{BN}_{\text{Full}})/L(\text{data} \mid \text{BN}_{\text{Full}-1})\right]$). Thus, LLR metrics indicated the relative improvement in model accuracy and precision due to the inclusion of prior knowledge of a single node in an uninformed BN (e.g., Figure S1), and the relative loss in model accuracy and precision due to the loss of prior knowledge of a single node in a well-informed BN, respectively. These LLR metrics, then, provide a measure of the influence of each parent node for predicting foredune morphology metrics and change in elevation.

RMSE provides a measure of absolute error between observed and predicted foredune metrics, given different combinations of prior knowledge. Correspondingly, for the null GBN model (no prior knowledge; means only model), the RMSE measures the standard error of the node. Finally, Efron's pseudo R^2 values provide a standardized measure of error, calculated as

$$\text{pseudo } R^2 = 1 - \frac{\sum_{i=1}^{N} (y_i - \widehat{y}_i)^2}{\sum_{i=1}^{N} (y_i - \overline{y})^2}$$

where N is the number of observations in the model, y is the target variable, y_i is the ith observation of y, $\overline{y}$ is the mean of all y_i, and $\widehat{y}_i$ is the maximum a posteriori estimate predicted by the BN for the ith observation. This pseudo R^2 metric is a standardized measure of absolute error, such that the pseudo R^2 for a model given prior knowledge is equivalent to the $1 - \text{RMSE}_{\text{post}}{}^2/\text{RMSE}_{\text{Null}}{}^2$. A high pseudo R^2 values indicates either that prior knowledge of parent variables is strongly predictive of the variable of interest (analogous to a high signal-to-noise ratio because of a strong signal) or that the variable has low variance (analogous to a high-signal-to noise ratio because of minimal noise). Consequently, the underlying degree of variability (i.e., noise) in ecological and morphological conditions encompassed within this study will influence the value of the pseudo R^2 statistic.

For the BN models, we calculated LLR, RMSE, and pseudo R^2 skill metrics for predicting foredune morphometrics (d_t elevation, d_c elevation, d_{face} slope, and foredune width) and foredune change (Δ elevation) based on different combinations of updated (prior) knowledge for nonforedune morphology nodes. All metrics were calculated using the complete data sets for the purpose of measuring descriptive BN performance (Beuzen et al., 2018). From these comparisons, we identify which beach and vegetation characteristics most closely relate to foredune morphology and its change.

2.4. Supporting Statistical Analyses

Although the foredune change BNs model elevation change at individual points on the foredune face, the BNs do not capture foredune volumetric changes over time. So we performed an additional linear mixed model to examine how beach sediment budgets and backshore slope relate to foredune volumetric change between 2012 and 2014. We estimated the volume of foredune sediment in the cross-shore profile of each transect in 2012 and 2014, approximated as regions of the foredune exceeding 4-m elevation above LMSL and calculated foredune volumetric change. We then compared log (volumetric change) against the 2012 log (backshore slope) and the log (shoreline change rate+2; enabling log transformation of slightly negative SCRs) using a linear mixed model, with a random intercept grouped by sublittoral cell. Mixed modeling was performed using nlme v3.1 (Pinheiro et al., 2014) in R.

3. Results

3.1. Foredune Morphology of Pacific Northwest Dunes

3.1.1. Sample Space and Likelihood Functions

The likelihood function for each node of the foredune morphology BNs illustrates the diverse ecological and geomorphological conditions that our dune data set encompassed (Figure S2). For example, SCR varied from −1.6 to 9.2 m/year (median: 0.7 m/year), encompassing both rapidly accreting and modestly eroding beaches; shoreface slope varied from 0.003 to 0.018 (median: 0.011); backshore slope varied from 0.01 to 0.21 (median: 0.05), representing dissipative to intermediate-reflective beach types (Wright & Short, 1984); beachgrass densities varied between 0 and 516 tillers/m^2 (median: 74 tillers/m^2); d_{face} slope varied between 0.06 and 0.75 (median: 0.25), foredune width between 8.3 and 188.1 m (median: 41.5 m); d_t elevation ranged from 3.0 m to 10.9 m above LMSL (median: 5.0 m); and d_c elevation ranged between 5.2 and 18.1 m above LMSL (median: 9.6 m).

3.1.2. Skill Assessments

Comparison of skill metrics (i.e., RMSE, LLR, and pseudo R^2) between alternative foredune morphology BN structures (Figure 2) showed that *Ammophila arenaria* and *A. breviligulata* are associated with distinct foredune morphologies. Skill metrics for d_c elevation, d_{face} slope, and foredune width were higher for the Morphology-CLGN$_{\text{species}}$ network that distinguished between the two *Ammophila* species (Figure 2b) as compared to the Morphology-GBN$_{\text{combined}}$ network that treated the species as functionally equivalent (Figure 2a and Table 1). For example, the LLR value of 7.1 for d_{face} slope indicates that the likelihood of the observed data given the CLGN$_{\text{species}}$ model is $e^{7.1} = 1{,}212$ times as likely as the data under the

Table 1
Comparison of Bayesian Network Skill Metrics for Two Foredune Morphology Bayesian Networks That Either Combined Beachgrass Species (Morphology-GBN$_{combined}$; Figure 2a) or Treated Them Separately (Morphology-CLGN$_{species}$; Figure 2b)

Predicted foredune morphometric	Model	RMSE (Lower is better)	Pseudo R^2 (Higher is better)	LLR $\log\left(\frac{L(D\|\mathrm{BN_{Full}})}{L(D\|\mathrm{BN_{Null}})}\right)$	LLR model comparison $\log\left(\frac{L(D\|\mathrm{CLGN_{species}})}{L(D\|\mathrm{GBN_{combined}})}\right)$
d_c elevation	GBN$_{combined}$	0.193	0.346	51.8	
	CLGN$_{species}$	0.192	0.353	53.6	1.8
d_t elevation	GBN$_{combined}$	0.211	0.383	59.5	
	CLGN$_{species}$	0.211	0.383	59.1	−0.4
d_{face} slope	GBN$_{combined}$	0.344	0.47	78.1	
	CLGN$_{species}$	0.330	0.504	85.2	7.1
d_{face} width	GBN$_{combined}$	0.619	0.111	14.4	
	CLGN$_{species}$	0.585	0.209	28.2	13.8

Note. The three skill metrics (root-mean-square error [RMSE]; pseudo R^2; log-likelihood ratio [LLR]) allowed for comparison of descriptive accuracy and precision among hypothesized network structures.

GBN$_{combined}$ model, and the corresponding change in pseudo R^2 value from 0.47 to 0.503 shows that inclusion of species in the network results in a slight increase in the accuracy of d_{face} slope predictions. Consequently, there is strong evidence for an association between *Ammophila* species identity and d_c elevation, d_{face} slope, and foredune width based on LLR and pseudo R^2 values. However, there was negligible evidence that d_t elevation varied between *Ammophila* species.

When exploring the relative influence of variables for predicting foredune morphometrics, prior knowledge of backshore slope, beachgrass density, and SCR acted as the strongest predictors of d_c elevation at these sites (Figure 4). Based on comparisons of the Morphology-CLGN$_{species}$ with full knowledge to that with knowledge of all but one predictor (LLR = $\log[L(\text{data} \mid \mathrm{BN_{Full}})/L(\text{data} \mid \mathrm{BN_{Full-1}})]$) and comparisons of CLGN$_{species}$ with one predictor only to a null model (LLR = $\log[L(\text{data} \mid \mathrm{BN_{Null+1}})/L(\text{data} \mid \mathrm{BN_{Null}})]$), we found that backshore slope, SCR, and beachgrass density increased the LLR of the d_c elevation node by 35.6–41.8, 8.4–11.3, and 3.7–6.5, respectively, indicating strong evidence that these variables are associated with d_c elevation. Prior knowledge of dominant species, however, decreases the LLR by 4.5, indicating that the CLGN poorly predicts d_c elevation from dominant species (when shoreface slope is known).

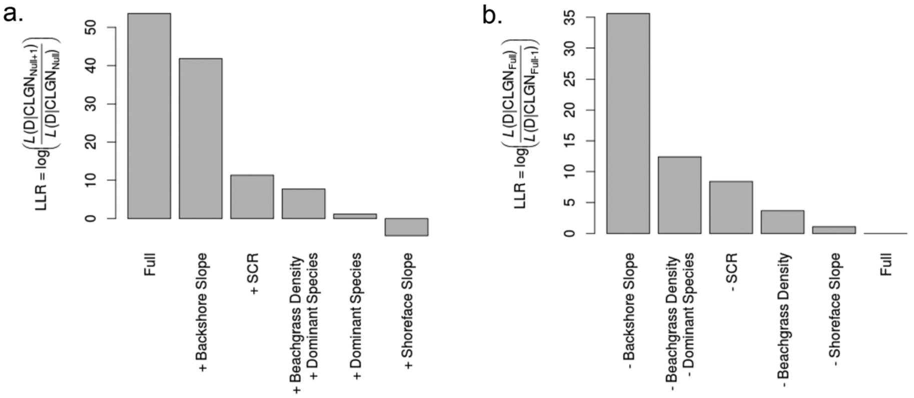

Figure 4. Relative influence of predictor variables on foredune crest (d_c) elevations (Morphology-CLGN$_{species}$; Figure 2b), based on log-likelihood ratios (LLR). LLR values were calculated (a) for inclusion of prior information on a single node relative to a null network and (b) for inclusion of full knowledge (i.e., knowledge of all node values except d_t elevation, d_{face} width, d_{face} slope, and d_c elevation) relative to a network lacking prior knowledge of a single node. LLR values indicate the relative improvement in descriptive accuracy and precision when prior knowledge of a variable is included for predicting d_c elevations.

Foredune toe elevation was strongly associated with backshore slope (LLR: 47.8–53.9) and SCR (LLR: 1.2–9.7). Among d_{face} slope predictors, there is strong evidence that backshore slope and shoreface slope relate to d_{face} slope (LLR: 42.3–64.8 and 4.2–5.6, respectively). Dominant beachgrass species was also strongly associated with d_{face} slope (LLR: 36.4–41.7), but it is unclear whether this relationship is because of the beachgrasses themselves or covariation with other variables (e.g., shoreface slope). Inclusion (exclusion) of both beachgrass density and dominant species as prior information provided little change in d_{face} slope descriptive skill as compared to inclusion (exclusion) of dominant species alone (LLR: −0.8–0.6; Tables S7 and S8). Finally, foredune width was associated with dominant species (LLR: 20.3–36.5) and beachgrass density (LLR: 5.0), whereas most other predictors provided little improvement in descriptive accuracy and precision.

3.1.3. Geomorphological Determinants of Foredune Morphology

Backshore slope and SCR were strongly associated with variation in foredune morphometrics (Figure 2a). SCR was directly negatively associated with backshore slope and d_c elevation (red arrow) and positively associated with d_t elevation (black arrow). SCR was also indirectly, negatively associated with foredune width and d_{face} slope (via backshore slope). Backshore slope was positively associated with foredune width, foredune slope, d_t elevation, and d_c elevation (black arrows). Together, these results suggest that locations with high SCR exhibit shallow-sloped backshore zones and foredunes that are shallow-sloping and short. In contrast, locations with low SCR exhibit steeper-sloped backshore zones, with steeper, wider, and taller foredunes.

3.1.4. Ecological Determinants of Foredune Morphology

Beachgrass density similarly influenced foredune morphometrics. When *Ammophila* species were pooled into a single random variable (Foredune Morphology-GBN$_{\text{combined}}$; Figure 2a), beachgrass density was directly, positively related to foredune width (black arrow) and indirectly positively related to d_c elevation. This pattern suggests that as beachgrass density increases, foredunes become wider and taller. When considered separately (Foredune Morphology-CLGN$_{\text{species}}$; Figure 2b), *A. breviligulata* density exhibited a positive direct relationship with foredune width (black arrow), a negative indirect relationship with d_{face} slope, and a predominantly positive indirect relationship with d_c elevation. In contrast, *A. arenaria* density exhibited a positive direct relationship with d_{face} slope (black arrow) and a positive indirect relationship with d_c elevation. This pattern suggests that as *A. breviligulata* density increases, the foredune becomes wider, more shallow sloping, and taller; for *A. arenaria*, as density increases, the foredune becomes steeper and taller.

3.2. Change in Foredune Morphology of Pacific Northwest Dunes

3.2.1. Sample Space and Likelihood Functions

Similar to the foredune morphology analyses above, the foredune change BNs encompassed varied ecological and geomorphological conditions (Figure S3). SCR varied from −1.5 to 8.3 m/year (median: 0.9 m/year); shoreface slope varied from 0.005 to 0.018 (median: 0.008); backshore slope varied from 0.01 to 0.10 (median: 0.04); quadrat elevations varied from 2.5 to 17.9 m above LMSL (median: 6.7 m); beachgrass densities ranged from 0 and 556 tillers/m^2 (median: 34 tillers/m^2); change in beachgrass density (log (density$_{2014}$/density$_{2012}$)) ranged from 99.2% decrease to a 413% increase (median: 15.5% increase); and change in elevation (indicative of sand accretion) between 2012 and 2014 within quadrats ranged from −1.1 and 1.7 m (median: 0.4 m).

3.2.2. Skill Assessments

Comparison of the skill metrics between the Accretion-CLGNs (Figure 3) showed that *A. arenaria* and *A. breviligulata* differed in their influence on sand accretion. The BN that distinguished between *A. arenaria* and *A. breviligulata* (Accretion-CLGN$_{\text{species}}$; Figure 3b) exhibited lower RMSE, higher pseudo R^2, and higher LLR for predicting elevation change along d_{face} between 2012 and 2014 than the BN that combined both beachgrass species (Accretion-CLGN$_{\text{combined}}$; Figure 3a and Table S9). Correspondingly, based on a LLR comparison of network structure where LLR = $\log [L(\text{data} \mid \text{CLGN}_{\text{species}})/L(\text{data} \mid \text{CLGN}_{\text{combined}})]$, the LLR of 4.8 indicates that the data are 120 times more likely under the CLGN$_{\text{species}}$ than under the CLGN$_{\text{combined}}$ model. Consequently, there is strong evidence that inclusion of species-specific information improved model accuracy and precision and that the two beachgrass species differed in their influence on foredune elevation change (i.e., sand accretion).

When exploring the relative importance of variables for predicting elevation change along d_{face}, prior knowledge of both vegetation and geomorphological variables provided strong predictors of this change (Figure 5).

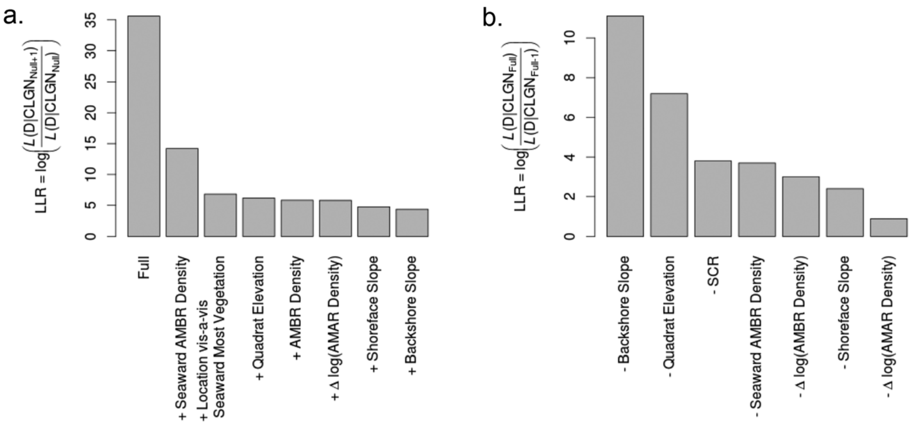

Figure 5. Relative influence of predictor variables on quadrat elevation change (Accretion-CLGN$_{species}$; Figure 3b), based on log-likelihood ratios (LLR). LLR values were calculated (a) for inclusion of prior information on a single node relative to a null network and (b) for inclusion of full knowledge (full) relative to a network lacking prior knowledge of a single node. LLR values indicate the relative improvement in descriptive accuracy and precision when prior knowledge of a variable is included for predicting quadrat elevation change.

There is strong evidence that elevation, backshore slope, shoreface slope, and SCR influence elevation change (Tables S10 and S11). Among vegetation variables, seaward *A. breviligulata* density most strongly influenced elevation change (LLR: 3.7–13.9), and changes in *A. arenaria* density (as measured by the log fold-change in tiller density between 2014 and 2012) were also associated with elevation change (LLR: 0.9–5.8). The log fold-change in *A. breviligulata* tiller density was weakly associated with elevation change (LLR: −1.0–3.2).

3.2.3. Geomorphological Determinants of Foredune Change

Based on the Accretion-CLGN$_{species}$ (Figure 3b), shoreface slope, backshore slope, and SCR exhibited direct, positive relationships with elevation change (black arrows), but SCR also exhibited an indirect, negative relationship with elevation change (via backshore slope). These relationships suggest that foredunes along steep sloping backshore environments accreted sand more rapidly per unit area than foredunes along shallow-sloping backshore environments, given similar SCR conditions (Figure S4). The impact of SCR on elevation change is characterized by two counteracting processes: higher SCR (i.e., prograding beaches) was directly associated with increased vertical sand accretion yet was also associated with lower backshore slopes and by extension, reduced vertical sand accretion (Figure S5). Initial elevation exhibited negative, direct relationship with elevation change, suggesting that higher elevation regions on d_{face} accrete less sand than low elevation regions. Finally, the complementary linear mixed model analysis show that SCR was positively associated with foredune volumetric change ($F_{1,58} = 11.0$, $p = 0.002$), whereas backshore slope was negatively associated with volumetric change ($F_{1,58} = 31.0$, $p < 0.0001$).

3.2.4. Ecological Determinants of Foredune Change

3.2.4.1. Vegetation Growth Patterns

Ammophila arenaria and *A. breviligulata* exhibited differing growth patterns along d_{face}, based on Accretion-CLGN relationships (Figure 3b). In locations where *A. arenaria* was dominant, the log fold-change in *A. arenaria* tiller density between 2012 and 2014 was negatively related to its 2012 density and also its 2012 landward density (red arrows). Specifically, for every doubling of initial *A. arenaria* tiller density and initial landward tiller density, the fold-change in *A. arenaria* density between 2012 and 2014 decreased by 2% and 12%, respectively, when holding other variables constant.

Ammophila breviligulata exhibited a markedly different growth pattern. The log fold-change in *A. breviligulata* tiller density between 2012 and 2014 was directly, positively related to initial landward and seaward *A. breviligulata* density (black arrows in Figure 3b) and negatively related to initial *A. breviligulata* density at that particular quadrat (red arrow). For example, for every doubling of initial *A. breviligulata* density, the fold-change in *A. breviligulata* tiller density decreased by 41% along the vegetated portion of d_{face}, when holding other variables constant. In contrast, for every doubling of neighboring landward and seaward tiller density in 2012, the fold-change in *A. breviligulata* tiller density increased by 36% and 15%, respectively.

3.2.4.2. Differential Influence on Foredune Change

Ammophila arenaria and *A. breviligulata* further differed in their effect on elevation change over time, based on the Accretion-CLGN$_{\text{species}}$. The log fold-change in tiller density between 2012 and 2014 (indicative of tiller production) for both *A. arenaria* and *A. breviligulata* were directly, positively associated with elevation gain (black arrows). Seaward *A. breviligulata* was directly, negatively associated with elevation change (red arrow) and indirectly, positively associated with elevation change (via Δlog (tiller density)). For *A. arenaria*, then, each doubling of tiller density between 2012 and 2014 was associated with a mean increase in elevation of 0.034 m during the same period, when other variables are held constant. For *A. breviligulata*, a doubling of density between 2012 and 2014 produced a 0.026-m elevation gain. However, elevation gain from new *A. breviligulata* tiller production was also limited by seaward *A. breviligulata*, which reduced elevation by 0.032 m for every doubling of seaward beachgrass density, when other variables were held constant. Consequently, while production of *A. breviligulata* tillers on d_{face} may facilitate deposition, their impact is counteracted by seaward beachgrasses, which inhibit deposition on landward portions of d_{face}.

4. Discussion

In this study, we developed two sets of Bayesian network models to (1) evaluate which factors are important in determining foredune morphology and changes to foredune morphology and (2) investigate whether species-specific differences in density and growth form between *A. arenaria* and *A. breviligulata* are important to these patterns. For examining determinants of foredune morphology (H_1), we found that backshore slope, SCR, dominant *Ammophila* species, and beachgrass density were the best predictors of foredune morphometrics (Figure 4 and Tables S7 and S8). Parameterization of the BNs further showed that locations with high SCRs exhibit shallow-sloped backshores, and short, shallow-sloping foredunes. Beachgrass density, in turn, altered the height, width, and slope of foredunes (H_2), but its mode of impact varied between *A. arenaria* and *A. breviligulata* (H_3-H_4). As *A. arenaria* density increased, foredunes became steeper and taller but had little influence on foredune width; in contrast, with increasing *A. breviligulata* density, foredune height still increased, but foredunes become wider and more shallow sloped.

An examination of sand deposition patterns at locations along the foredune face (d_{face}; between d_t and d_c) over a 2-year period showed that sand deposition was most strongly influenced by species-specific patterns of vegetation growth, backshore slope, SCR, and initial elevation (Figure 5 and Tables S10 and S11). Based on the Accretion-CLGNs, locations with high SCR and shallow-sloping backshore zones experienced higher rates of elevation gain on the foredune face, indicative of sand accretion (H_1). We further found that sand accretion was concentrated at lower elevations and gradually decreased as elevation increased. Plant species identity (H_3, H_4) and tiller density (H_2, H_4) also altered patterns of deposition: although initial plant density did not directly alter deposition rates, locations in which *Ammophila* density increased over the 2-year period had heightened accretion relative to locations where density did not change. In contrast, seaward-occurring *A. breviligulata* inhibited sand accretion on landward portions of the foredune face. Finally, the Accretion-CLGNs demonstrated that *A. arenaria* and *A. breviligulata* exhibit differing growth patterns, with substantial morphodynamic consequences.

Although our analyses encompass many determinants of foredune ecomorphodynamics, several other factors may also influence foredune development that were not accounted for in these Bayesian networks. For example, wind speed, fetch length, variations in wave amplitude, period, and direction, and short-timescale variations in shoreline change rates affect beach-dune morphodynamics (e.g., Bauer et al., 2009; Ruggiero et al., 2005; Walker et al., 2017). Correspondingly, wave exposure, salt spray, water availability, temperature, and nutrient availability can alter the distribution and abundance of plants on beaches and dunes (Barbour et al., 1985) and may resultantly alter how dunes morphologically evolve (e.g., Hesp, 1989; Mathew et al., 2010).

4.1.1. Geomorphological Regulation of Foredune Morphodynamics

Empirical studies of foredune geomorphology show that foredune size is associated with beach type, whereby dissipative beaches (i.e., wide, shallow sloping, and fine sediment grain size) typically have larger foredunes than reflective beaches (Duran & Moore, 2013; Hesp, 1988; Short & Hesp, 1982). Corresponding observations and conceptual models suggest that dissipative beaches may offer a higher sand supply to dunes because of elevated wave-driven sediment supply to the beach and/or fetch length, thereby generating enhanced aeolian sediment fluxes from beaches to foredunes, making them larger (Cohn et al., 2018; Houser & Mathew, 2011; Saye et al., 2005; Short & Hesp, 1982). Similarly, wider beaches may promote the formation of taller dunes than narrow beaches due to a negative feedback between sand flux and topography that arises from onshore wind deflection by the foredune (Duran & Moore, 2013). However, this direct relationship between beach morphology and foredune morphology is overly simplified, as there are numerous counterexamples of dissipative beaches with high sediment supplies and short foredunes (Hacker et al., 2012; Miot da Silva & Hesp, 2010; Ruggiero et al., 2005). Our findings further illustrate that the relationship between beach type, sediment supply, and foredune morphology is complex and context dependent.

Our models show that low angle, wide, dissipative beach conditions were associated with shorter foredunes and reduced elevation gain as compared to intermediate and intermediate-reflective beaches, when holding other variables constant (Figures 3 and 4, and S4). While SCR may partly confound this relationship as it is negatively correlated with backshore slope, we find that this relationship between backshore slope, foredune morphology, and sand accretion remains, even when holding SCR constant. Given that we also observed a larger change in foredune volume on dissipative beaches with high SCR, it seems that dissipative conditions may be associated with a higher aggregate rate of sand accretion across the entire foredune profile but may not necessarily produce more rapid foredune elevation gain or even taller foredunes.

Within our system, SCR was directly associated with higher sand deposition on the dune face (Figure S5), indicating that higher supply of sediment to the beach enhances the supply of sand to the dune (Figure 3b). Yet locations with high SCR were also associated with shorter foredunes (Figure 2; Hacker et al., 2012; Moore et al., 2016). These morphodynamic patterns are broadly consistent with beach-dune sediment budget models by Psuty (1988) and Pye (1990). Psuty (1988) proposed that foredune development depends upon the sediment supply to the beach and sediment supply to the dune, while Pye (1990) included availability of wind energy and sand-trapping vegetation efficacy as additional modifiers of foredune development. Under both beach-dune sediment budget models, foredune development is maximized under near-neutral beach-dune budgets, where a net-neutral supply of sand to the beach provides a net-positive supply of sand to the foredune: over years, shoreline and foredune position remain stable, allowing sand to accumulate along the foredune crest, resulting in the development of tall foredunes. In contrast, as shoreline progradation rates increase, foredune dimensions gradually decrease as they instead form a series of small foredune ridges (Moore et al., 2016; Psuty, 2008). For example, in the Columbia River Littoral Cell, which encompasses many of the progradational sites in this study, beach sediment budgets are mostly positive and have produced an average SCR of 1.1 to 3.7 m/year. Between 1997 and 2014, this positive sediment budget has resulted in the formation of one to two new foredune ridges (Ruggiero et al., 2016).

It is unclear why backshore slope is positively related to both foredune height and changes in foredune elevation, but several processes may contribute to this observed pattern. First, the regression analysis indicates that SCR is positively associated with volumetric change across the entire foredune cross-shore profile, whereas backshore slope is negatively associated with foredune volumetric change. So it is likely that narrower, steeper beaches may provide a lower volumetric supply of sediment to the foredune. Nevertheless, because narrow and steep beaches often have tall and narrow foredunes, this smaller volume of sediment is likely to be deposited over a smaller region in the cross shore. This difference could give rise to a greater elevation gain along the foredune profile, despite the overall lower volumetric sediment supply. Second, Short and Hesp (1982) hypothesize that wider beaches promote greater sediment supply and taller dunes because of fetch limitations on narrower, steep beaches. In the Pacific Northwest, though, formative winds primarily arise from oblique wind directions that vary seasonally. Consequently, beach width and slope may insufficiently capture fetch and overall aeolian sediment transport to the dune. Third, it is possible that our measurement of SCR may not reflect the most relevant timescale for dune formation and sediment accretion. This study used measurements of shoreline change over two to three decade timescales. However, shorelines vary seasonally and interannually due to spatiotemporal variations in sediment budgets, wind speed and direction, wave conditions, storms, El Niño–Southern Oscillation, and other forcing that we were unable to include in these BNs. Thus, some disparities in timescale, response, and unquantified forcing may obscure the relationship between backshore slope, rates of shoreline change, and dune development and may also contribute to the high uncertainty and lower pseudo R^2 values of these BNs.

4.1.2. Ecological Regulation of Foredune Morphodynamics

The morphodynamics of U.S. Pacific Northwest foredunes are further influenced by vegetation dynamics, including plant density, plant morphology, and growth patterns. Historically, Pacific Northwest coastal foredunes were dominated by endemic grasses (*Elymus mollis*) and forbs (e.g., *Abronia latifolia* and *Lathyrus littoralis*) that grew in sparse assemblages (Wiedemann, 1984). This low vegetation cover, combined with a high sand supply and seasonal wind patterns allowed for the formation of dune hummocks, barchan dunes, transverse ridges, and oblique ridges (Cooper, 1958). However, with the introductions of densely growing *A. arenaria* and *A. breviligulata* as sand stabilizers and their subsequent spread throughout the region, the historically open-sand dune system transitioned to a highly vegetated, stabilized system of shore-parallel, linear foredunes (Wiedemann & Pickart, 1996).

Although both *Ammophila* species transformed Pacific Northwest foredunes, *Ammophila breviligulata*-dominated foredunes are shorter, wider, and more shallow-sloping than *A. arenaria*-dominated foredunes (Hacker et al., 2012; Seabloom & Wiedemann, 1994). Some foredune morphological differences likely result from spatially correlated sediment supply patterns, as has been previously documented (Hacker et al., 2012; Zarnetske et al., 2015). Nevertheless, Hacker et al. (2012) posited that subtle differences in the traits of these similar-looking *Ammophila* species may also produce distinct foredune morphotypes. Thus, we further hypothesized that increasing beachgrass stem density will be associated with taller and narrower foredunes (H_2), that inclusion of species-specific stem density variables will improve the accuracy and precision of the BNs for predicting foredune morphology (H_3), and that *A. breviligulata* stem density will be more positively associated with foredune height than *A. arenaria* stem density due to species-specific differences in stem morphology (H_4).

4.1.2.1. Influence of Ammophila on Foredune Morphodynamics

While backshore slope and SCR predominantly predicted foredune morphological variation, beachgrass density also contributed (Figure 4 and Tables S7 and S8) and was positively associated with wider and taller foredunes. Correspondingly, rates of sand accretion along d_{face} were primarily associated with the log fold-change in beachgrass density and backshore slope (Figure 3 and Table S10) and are consistent with observed and modeled aeolian dynamics along vegetated foredunes. Field experiments by Hesp (1984) and Arens et al. (2001) show that increasing vegetation density is associated with greater sediment deposition and the development of taller (although narrower) incipient dunes.

Foredune morphology and sand accretion along d_{face} also differed among the *Ammophila* species, even when accounting for variations in sediment supply. In our models, inclusion of distinct nodes for the two *Ammophila* species increased log-likelihood ratios (LLRs; i.e., improved accuracy and/or precision of model predictions) for d_c elevation, d_{face} slope, and foredune width (Table 1). Separating the *Ammophila* species into separate nodes similarly improved BN performance for predicting elevation change along the dune face over time (Table S9). Therefore, our results were consistent with previous research showing distinctive geomorphologies between *A. arenaria*- and *A. breviligulata*-dominated foredunes.

Hacker et al. (2012) hypothesized that subtle differences in the density, morphology, and growth form of *A. arenaria* and *A. breviligulata* may facilitate the formation of species-specific foredune geomorphologies. For example, *A. breviligulata* tillers are 30% wider and 15% taller than *A. arenaria* tillers and induce greater sediment deposition per tiller than *A. arenaria* in a wind tunnel (Zarnetske et al., 2012). Yet *A. arenaria* exhibits a vertical, "phalanx" growth form and grows at a higher density than *A. breviligulata*, which exhibits a laterally expansive "guerilla" growth form. These differences in density potentially facilitate faster vertical dune growth on *A. arenaria*-dominated foredunes because of their higher sand capture efficiency (volume of deposited sand per unit area).

However, our models indicate that grass density alone does not explain the species-specific differences in foredune morphology. Our foredune morphology model (Figure 2b) indicates that increasing *A. arenaria* density was associated with steeper and taller foredunes, whereas increasing *A. breviligulata* density was associated with wider, albeit shallow sloping, and taller foredunes. Even so, when we examined how the species differed in their rates of sand accretion (Figure 3b), initial beachgrass density was not directly associated with sand accretion for either species and *A. arenaria* only accreted marginally more sand per doubling of new tillers than *A. breviligulata*, given similar conditions. Thus, neither differences in density nor beachgrass tiller morphology explain why *Ammophila* species exhibit differing foredune shapes. However, differences

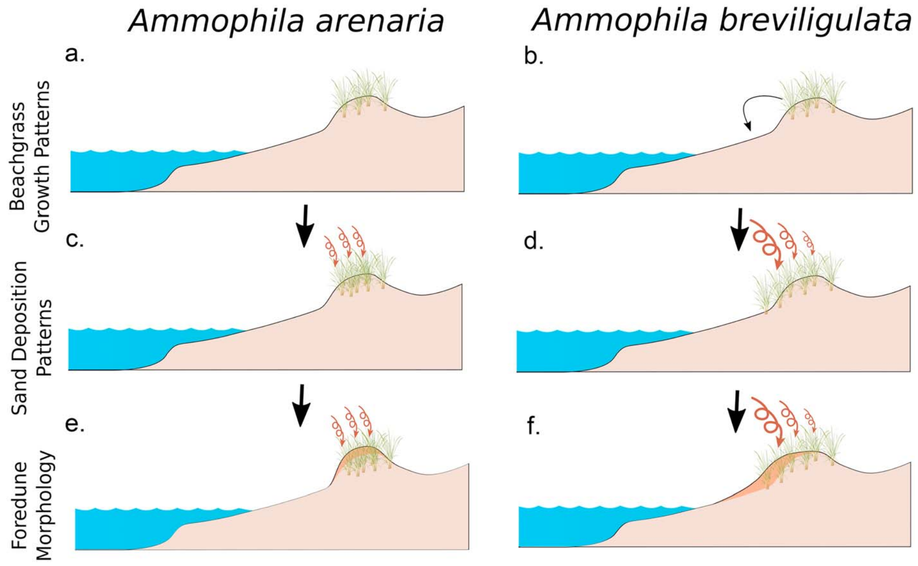

Figure 6. Illustration of proposed mechanism to explain differences in sand accretion and foredune morphology patterns between *A. arenaria* and *A. breviligulata*. Growth patterns (a and b): *Ammophila breviligulata* exhibits greater lateral growth than *A. arenaria*, resulting in greater seaward expansion of *A. breviligulata* (black arrow; Figure 3b). Sand deposition patterns (c and d): *Ammophila breviligulata* exhibits higher sand deposition on the leading edge of the vegetated dune, where new growth is occurring, while sand deposition on landward regions is inhibited by existing grasses. *Ammophila arenaria* exhibits more diffuse sand deposition where new growth is occurring. Foredune morphology (e and f): Due to both growth and sand deposition patterns, *A. breviligulata*-dominated dunes exhibit greater seaward expansion of the foredune, whereas *A. arenaria* exhibits greater vertical dune growth. Correspondingly, *A. breviligulata* abundance is associated with shallow-sloped, wide foredunes, while *A. arenaria* growth patterns are associated with steeper sloped, taller foredunes (Figure 2b).

in growth form provides another explanation for species-specific variations in foredune morphology (Hacker et al., 2012). *Ammophila breviligulata* exhibits a higher rate of lateral growth than *A. arenaria*, with observed rates of lateral propagation of >3 m/year and <1 m/year, respectively (Baye, 1990; Keijsers et al., 2015; Maun, 1985). Correspondingly, *A. breviligulata* responds to high rates of sand burial by increasing horizontal tiller production, thereby enhancing its lateral growth, whereas *A. arenaria* responds by enhancing vertical tiller growth to outpace sand burial (resulting in its high density, clumped growth form; Zarnetske et al., 2012). Based on our analyses, these differences in growth form may be responsible for species-specific differences in foredune morphology (Figure 6). In the Accretion-CLGN$_{\text{species}}$ model, we observed that the fold-change in tiller production for *A. breviligulata* was positively associated with its initial density in adjacent landward and seaward quadrats, whereas *A. arenaria* exhibited a comparatively weak positive relationship with its landward quadrat (Figure 3b). This pattern is consistent with lateral propagation by *A. breviligulata* into neighboring areas over the 2-year observation period, but limited lateral expansion by *A. arenaria* (Figures 6a and 6b).

The species-specific differences in lateral growth rate, when combined with density-dependent growth patterns, alter sand deposition on the foredune. Sand accretion was enhanced in regions where tiller production for either species was high (Figures 3 and 6c and 6d). For example, *A. breviligulata* tiller production was concentrated at the seaward margin of the foredune (Figure 6d), resulting in increased accretion near the foredune toe and reduced vertical accretion on the foredune crest (Figure 6f). This cross-shore gradient in *A. breviligulata* tiller production and sand deposition, then, primarily increases foredune width (Figure 3b). In contrast, *A. arenaria* tiller production occurred throughout the foredune face and crest (Figure 6c), resulting in sand deposition on both the foredune face and crest (Figure 6e). Given that *A. arenaria* also exhibits slow lateral propagation, this suggests that *A. arenaria*-dominated foredunes may exhibit slow lateral expansion of the foredune, resulting in a steeper, narrower foredune (Figure 3b).

Existing foredune ecomorphodynamic models may provide additional insight into the short-term and long-term vegetation and sediment dynamics of this system. At short timescales, field and wind-tunnel experiments by Hesp (1983), Arens et al. (2001), and Zarnetske et al. (2012) demonstrate that higher vegetation densities induce greater sediment accretion and may produce taller and narrower incipient dunes as a result of increasingly localized sediment deposition. However, these short-term experiments do not consider the influence of spatiotemporal changes to the spatial arrangement of vegetation and its interaction with sand supply on dune development, as occurred throughout our observational study. For example, long-term observation and simulation of foredune development have shown that changes in vegetation distributions on a beach or dune over time can create complex topographic features (Goldstein et al., 2017; Hesp, 1984). Given that different plant species exhibit varying capacities for (and distinct strategies for) colonizing the backshore, surviving disturbance (e.g., storms), propagating, modifying the wind field, and responding to sand burial (e.g., Barbour et al., 1985; Maun, 1998; Zarnetske et al., 2012), the distribution and abundance of vegetation on the backshore will depend upon a combination of which plant species are present and their responses to storms, shoreline change, and other forcing. Because of this coupling between vegetation dynamics and dune development, species-specific plant traits are likely to produce distinct, complex behavior in dune development.

5. Conclusions

This study demonstrates the interactive contributions of beach sediment supply, beach morphology, and vegetation dynamics in shaping foredune development. Although inclusion of vegetation species identity and density measurements improved the accuracy and precision of the Bayesian networks for predicting foredune morphology and rates of sand accretion, backshore slope and beach sediment budget (i.e., SCR) remained the dominant factors for explaining variation in foredune morphology. At the finer-scale examination of foredune change over time, though, beachgrass species identity and density were among the strongest predictors of sand accretion. Thus, the use of descriptive Bayesian network analyses to demonstrate the relative contributions and interactions among vegetation growth patterns, beach sediment budgets, and beach and foredune morphology provides an effective tool for examining hypothesized mechanisms that might influence foredune development.

As this study suggests, the examination of ecomorphodynamic influences on foredune development is understudied but critical to our ability to understand the mechanisms shaping dune morphology. For example, while this and related studies (e.g., Zarnetske et al., 2012, 2015) examined grasses (e.g., *Ammophila* species and *E. mollis*) as dune builders, beach and dune plants exhibit a wide range of morphologies and life history strategies. Dune-forming plants also including prostrate annual and perennial forbs (e.g., *Glehnia littoralis* and *Lathyrus* species) and species that primarily propagate via seed and via rhizomes and stolons. These different morphologies, methods of propagation, life history strategies, and physiological tolerances may alter sand capture efficiency, seasonality and temporal variability in accretion, and rates of ecological and geomorphological recovery following storms. Finally, while our research on ecomorphodynamic feedbacks in the U.S. Pacific Northwest demonstrated impacts of beachgrasses on dune backing prograding and stable shorelines, most regions worldwide exhibit eroding shores (Bird, 1985) and are expected to suffer more severe erosion with accelerating sea-level rise (Elko et al., 2016). Future work that examines dune ecomorphodynamic processes on retreating shorelines and uses a variety of vegetation types would help to fill this knowledge gap.

Acknowledgments
Data used in the analyses presented here are found at https://doi.org/10.6073/pasta/976957e7e0b56ed836b67ea39c172eff (Biel et al., 2019). Special thanks to L. Carroll, D. Batson, J. Henderson, J. Wood, N. Cohn, and M. Conlin for assistance with data collection and field logistics. Funding was provided by grants from EPA STAR (R833836), NOAA COCA (NA15OAR4310243), and NOAA Oregon Sea Grant (NA14OAR4170064) to P. R. and S. D. H., an EPA STAR graduate fellowship (F13B20274) to R. G. B., and an OSU Provosts Distinguished Graduate Fellowship to R. G. B.

References

Akaike, H. (1974). A new look at the statistical model identification. *IEEE Transactions on Automatic Control*, *19*(6), 716–723. https://doi.org/10.1109/TAC.1974.1100705

Arens, S. M., Baas, A. C. W., Van Boxel, J. H., & Kalkman, C. (2001). Influence of reed stem density on foredune development. *Earth Surface Processes and Landforms*, *26*(11), 1161–1176. https://doi.org/10.1002/esp.257

Barbier, E. B., Hacker, S. D., Kennedy, C., Koch, E. W., Stier, A. C., & Silliman, B. R. (2011). The value of estuarine and coastal ecosystem services. *Ecological Monographs*, *81*(2), 169–193. https://doi.org/doi, https://doi.org/10.1890/10-1510.1

Barbour, M. G., de Jong, T. M., & Pavlik, B. M. (1985). Marine beach and dune plant communities. In B. F. Chabot, & H. A. Mooney (Eds.), *Physiological ecology of North American plant communities*, (pp. 296–322). Springer Netherlands. Retrieved from. https://doi.org/10.1007/978-94-009-4830-3_14

Bauer, B. O., & Davidson-Arnott, R. G. (2003). A general framework for modeling sediment supply to coastal dunes including wind angle, beach geometry, and fetch effects. *Geomorphology*, *49*(1–2), 89–108. https://doi.org/10.1016/S0169-555X(02)00165-4

Bauer, B. O., Davidson-Arnott, R. G. D., Hesp, P. A., Namikas, S. L., Ollerhead, J., & Walker, I. J. (2009). Aeolian sediment transport on a beach: Surface moisture, wind fetch, and mean transport. Contemporary Research in Aeolian Geomorphology 6th International

Conference on Aeolian Research (ICAR VI), 105(1–2). *Geomorphology*, *105*(1-2), 106–116. https://doi.org/10.1016/j.geomorph.2008.02.016

Baye, P. R. (1990). Comparative growth responses and population ecology of European and American beachgrasses (Ammophila spp.) in relation to sand accretion and salinity (PhD thesis). The Univ. of Western Ontario.

Beuzen, T., Splinter, K. D., Marshall, L. A., Turner, I. L., Harley, M. D., & Palmsten, M. L. (2018). Bayesian Networks in coastal engineering: Distinguishing descriptive and predictive applications. *Coastal Engineering*, *135*, 16–30. https://doi.org/10.1016/j.coastaleng.2018.01.005

Biel R. G., Hacker, S. D., Ruggiero, P., Carroll, L. (2019). United States Pacific Northwest surveys of coastal foredune topography and vegetation abundance, 2012-2014. Environmental Data Initiative. https://doi.org/10.6073/pasta/976957e7e0b56ed836b67ea39c172eff

Biel, R. G., Hacker, S. D., Ruggiero, P., Cohn, N., & Seabloom, E. W. (2017). Coastal protection and conservation on sandy beaches and dunes: Context-dependent tradeoffs in ecosystem service supply. *Ecosphere*, *8*(4), e01791. https://doi.org/10.1002/ecs2.1791

Bird, E. C. F. (1985). *Coastline changes. A global review*. Chichester, UK: Wiley and Sons.

Bloomberg, M. (2013). A stronger, more resilient New York. *The City of New York Special Initiative for Rebuilding and Resilience*, *2*(13), 2015.

Buijsman, M. C., Sherwood, C. R., Gibbs, A. E., Gelfenbaum, G., Kaminsky, G. M., Ruggiero, P., & Franklin, J. (2003). Regional sediment budget of the Columbia River littoral cell, USA. Open File Report 02-281 (No. OFR-2002-281). United States Geological Survey. Retrieved from http://pubs.usgs.gov/of/2002/of02-281/

Carignan, K. S., Taylor, L. A., Eakins, B. W., Warnken, R. R., Lim, E., & Medley, P. R. (2009). Digital elevation model of central Oregon coast: Procedures, data sources and analysis (No. NOAA Technical Memorandum NESDIS NGDC-25). Boulder, CO: U.S. Dept. of Commerce.

Carignan, K. S., Taylor, L. A., Eakins, B. W., Warnken, R. R., Sazonova, T., & Schoolcraft, D. C. (2009a). Digital elevation model of Garibaldi, Oregon: Procedures, data sources and analysis (No. NOAA Technical Memorandum NESDIS NGDC-16). Boulder, CO: U.S. Dept. of Commerce.

Carignan, K. S., Taylor, L. A., Eakins, B. W., Warnken, R. R., Sazonova, T., & Schoolcraft, D. C. (2009b). Digital elevation model of Port Orford, Oregon: Procedures, data sources and analysis (No. NOAA Technical Memorandum NESDIS NGDC-21). Boulder, CO: U.S. Dept. of Commerce.

Cohn, N., Ruggiero, P., de Vries, S., & Kaminsky, G. (2018). New insights on coastal foredune growth: The relative contributions of marine and aeolian processes. *Geophysical Research Letters*, *45*, 4965–4973. https://doi.org/10.1029/2018GL077836

Cooper, W. S. (1958). *Coastal sand dunes of Oregon and Washington*. Boulder, Colorado: Geological Society of America. https://doi.org/10.1130/MEM72-p1

Corenblit, D., Baas, A. C. W., Bornette, G., Darrozes, J., Delmotte, S., Francis, R. A., et al. (2011). Feedbacks between geomorphology and biota controlling Earth surface processes and landforms: A review of foundation concepts and current understandings. *Earth-Science Reviews*, *106*(3-4), 307–331. https://doi.org/10.1016/j.earscirev.2011.03.002

Denis, J.-B. (2013). rbmn: Handling Linear Gaussian Bayesian Networks. Retrieved from http://CRAN.R-project.org/package = rbmn

Duran, O., & Moore, L. J. (2013). Vegetation controls on the maximum size of coastal dunes. *Proceedings of the National Academy of Sciences*, *110*(43), 17217–17222. https://doi.org/10.1073/pnas.1307580110

Elko, N., Brodie, K., Stockdon, H., Nordstrom, K., Houser, C., McKenna, K., et al. (2016). Dune management challenges on developed coasts. *Shore & Beach*, *84*(1), 15.

Everard, M., Jones, L., & Watts, B. (2010). Have we neglected the societal importance of sand dunes? An ecosystem services perspective. *Aquatic Conservation: Marine and Freshwater Ecosystems*, *20*(4), 476–487. https://doi.org/10.1002/aqc.1114

Goldstein, E. B., Moore, L. J., & Durán Vinent, O. (2017). Lateral vegetation growth rates exert control on coastal foredune “hummockiness” and coalescing time. *Earth Surface Dynamics*, *5*(3), 417–427. https://doi.org/10.5194/esurf-5-417-2017

Gutierrez, B. T., Plant, N. G., & Thieler, E. R. (2011). A Bayesian network to predict coastal vulnerability to sea level rise. *Journal of Geophysical Research*, *116*, F02009. https://doi.org/10.1029/2010JF001891

Gutierrez, B. T., Plant, N. G., Thieler, E. R., & Turecek, A. (2015). Using a Bayesian network to predict barrier island geomorphologic characteristics. *Journal of Geophysical Research: Earth Surface*, *120*, 2452–2475. https://doi.org/10.1002/2015JF003671

Hacker, S. D., Zarnetske, P., Seabloom, E., Ruggiero, P., Mull, J., Gerrity, S., & Jones, C. (2012). Subtle differences in two non-native congeneric beach grasses significantly affect their colonization, spread, and impact. *Oikos*, *121*(1), 138–148. https://doi.org/10.1111/j.1600-0706.2011.18887.x

Hanley, M. E., Hoggart, S. P. G., Simmonds, D. J., Bichot, A., Colangelo, M. A., Bozzeda, F., et al. (2014). Shifting sands? Coastal protection by sand banks, beaches and dunes. *Coastal Engineering*, *87*, 136–146. https://doi.org/10.1016/j.coastaleng.2013.10.020

Hatzikyriakou, A., Lin, N., Gong, J., Xian, S., Hu, X., & Kennedy, A. (2015). Component-based vulnerability analysis for residential structures subjected to storm surge impact from Hurricane Sandy. *Natural Hazards Review*, *17*(1). https://doi.org/10.1061/(ASCE)NH.1527-6996.0000205

Hesp, P. A. (1983). Morphodynamics of incipient foredunes in New South Wales, Australia. In M. E. Brookfield, & T. S. Ahlbrandt (Eds.), *Developments in sedimentology*, (Vol. 38, pp. 325–342). Amsterdam: Elsevier. https://doi.org/10.1016/S0070-4571(08)70802-1

Hesp, P. A. (1984). *Foredune formation in southeast Australia. Coastal Geomorphology in Australia*, (pp. 69–97). Sydney: Academic Press.

Hesp, P. A. (1988). Surfzone, beach, and foredune interactions on the Australian south east coast. *Journal of Coastal Research*, *3*, 15–25. https://doi.org/10.2307/40928722

Hesp, P. A. (1989). A review of biological and geomorphological processes involved in the initiation and development of incipient foredunes. *Proceedings of the Royal Society of Edinburgh B*, *96*, 181–201.

Hesp, P. A. (2002). Foredunes and blowouts: Initiation, geomorphology and dynamics. *Geomorphology*, *48*(1–3), 245–268. https://doi.org/10.1016/S0169-555X(02)00184-8

Houser, C., Hapke, C., & Hamilton, S. (2008). Controls on coastal dune morphology, shoreline erosion and barrier island response to extreme storms. *Geomorphology*, *100*(3–4), 223–240. https://doi.org/10.1016/j.geomorph.2007.12.007

Houser, C., & Mathew, S. (2011). Alongshore variation in foredune height in response to transport potential and sediment supply: South Padre Island, Texas. *Geomorphology*, *125*(1), 62–72. https://doi.org/10.1016/j.geomorph.2010.07.028

Inman, D. L., & Frautschy, J. D. (1965). Littoral processes and the development of shorelines. In Coastal Engineering (p. 1006). American Society of Civil Engineers.

Intergovernmental Panel on Climate Change (IPCC) (2014). Climate change 2014: Synthesis report. Contribution of Working Groups I, II and III to the fifth assessment report of the Intergovernmental Panel on Climate Change. Geneva, Switzerland: IPCC.

Kass, R. E., & Raftery, A. E. (1995). Bayes factors. *Journal of the American Statistical Association*, *90*(430), 773–795. https://doi.org/10.1080/01621459.1995.10476572

Keijsers, J. G. S., De Groot, A. V., & Riksen, M. J. P. M. (2015). Vegetation and sedimentation on coastal foredunes. *Geomorphology*, *228*, 723–734. https://doi.org/10.1016/j.geomorph.2014.10.027

Keijsers, J. G. S., De Groot, A. V., & Riksen, M. J. P. M. (2016). Modeling the biogeomorphic evolution of coastal dunes in response to climate change. *Journal of Geophysical Research: Earth Surface*, *121*, 1161–1181. https://doi.org/10.1002/2015JF003815

Koller, D., Friedman, N., & Bach, F. (2009). *Probabilistic graphical models: Principles and techniques*. Cambridge, MA: MIT press.

Kriebel, D. L., & Dean, R. G. (1985). Numerical simulation of time-dependent beach and dune erosion. *Coastal Engineering*, *9*(3), 221–245. https://doi.org/10.1016/0378-3839(85)90009-2

Larson, M., Erikson, L., & Hanson, H. (2004). An analytical model to predict dune erosion due to wave impact. *Coastal Engineering*, *51*(8–9), 675–696. https://doi.org/10.1016/j.coastaleng.2004.07.003

Love, M., Friday, D., Grothe, P., Carignan, K., Eakins, B., & Taylor, L. (2012). Digital elevation model of Astoria, Oregon—Procedures, data sources, and analysis. Boulder, CO: U.S. Dept. of Commerce.

Mathew, S., Davidson-Arnott, R. G. D., & Ollerhead, J. (2010). Evolution of a beach–dune system following a catastrophic storm overwash event: Greenwich Dunes, Prince Edward Island, 1936–2005. *Canadian Journal of Earth Sciences*, *47*(3), 273–290. https://doi.org/10.1139/E09-078

Maun, M. A. (1985). Population biology of *Ammophila breviligulata* and *Calamovilfa longifolia* on Lake Huron sand dunes. I. Habitat, growth form, reproduction, and establishment. *Canadian Journal of Botany*, *63*(1), 113–124. https://doi.org/10.1139/b85-014

Maun, M. A. (1998). Adaptations of plants to burial in coastal sand dunes. *Canadian Journal of Botany*, *76*(5), 713–738. https://doi.org/10.1139/b98-058

Miot da Silva, G., & Hesp, P. A. (2010). Coastline orientation, aeolian sediment transport and foredune and dunefield dynamics of Moçambique Beach, Southern Brazil. *Geomorphology*, *120*(3–4), 258–278. https://doi.org/10.1016/j.geomorph.2010.03.039

Moore, L. J., Vinent, O. D., & Ruggiero, P. (2016). Vegetation control allows autocyclic formation of multiple dunes on prograding coasts. *Geology*, *44*(7), 559–562. https://doi.org/10.1130/G37778.1

Morton, R. A. (2002). Factors controlling storm impacts on coastal barriers and beaches: A preliminary basis for near real-time forecasting. *Journal of Coastal Research*, *18*(3), 486–501.

Mull, J., & Ruggiero, P. (2014). Estimating storm-induced dune erosion and overtopping along U.S. West Coast beaches. *Journal of Coastal Research*, *298*(6), 1173–1187. https://doi.org/10.2112/JCOASTRES-D-13-00178.1

Needham, C. J., Bradford, J. R., Bulpitt, A. J., & Westhead, D. R. (2007). A primer on learning in Bayesian networks for computational biology. *PLoS Computational Biology*, *3*(8), e129–e129. https://doi.org/10.1371/journal.pcbi.0030129

Pielke, R., Gratz, J., Landsea, C., Collins, D., Saunders, M., & Musulin, R. (2008). Normalized hurricane damage in the United States: 1900–2005. *Natural Hazards Review*, *9*(1), 29–42. https://doi.org/10.1061/(ASCE)1527-6988(2008)9:1(29)

Pinheiro, J., Bates, D., DebRoy, S., Sarkar, D., & R Core Team. (2014). nlme: Linear and nonlinear mixed effects models.

Plant, N. G., Flocks, J., Stockdon, H. F., Long, J. W., Guy, K., Thompson, D. M., et al. (2014). Predictions of barrier island berm evolution in a time-varying storm climatology. *Journal of Geophysical Research: Earth Surface*, *119*, 300–316. https://doi.org/10.1002/2013JF002871

Plant, N. G., & Stockdon, H. F. (2012). Probabilistic prediction of barrier-island response to hurricanes. *Journal of Geophysical Research*, *117*, F03015. https://doi.org/10.1029/2011JF002326

Poelhekke, L., Jäger, W. S., van Dongeren, A., Plomaritis, T. A., McCall, R., & Ferreira, Ó. (2016). Predicting coastal hazards for sandy coasts with a Bayesian Network. *Coastal Engineering*, *118*, 21–34. https://doi.org/10.1016/j.coastaleng.2016.08.011

Psuty, N. P. (1988). Sediment budget and dune/beach interaction. *Journal of Coastal Research*, *3*, 1–4. https://doi.org/10.2307/40928719

Psuty, N. P. (2008). The coastal foredune: A morphological basis for regional coastal dune development. In M. L. Martínez, & N. P. Psuty (Eds.), *Coastal Dunes: Ecology and Conservation*, (pp. 11–27). Berlin, Heidelberg: Springer Berlin Heidelberg. https://doi.org/10.1007/978-3-540-74002-5_2

Pye, K. (1990). Physical and human influences on coastal dune development between the Ribble and Mersey estuaries, northwest England. In K. F. Nordstrom, N. P. Psuty, & R. W. G. Carter (Eds.), *Coastal dunes: Form and process*, (pp. 339–359). Chichester: Wiley.

R Core Team. (2015). R: A language and environment for statistical computing. Vienna, Austria: R Foundation for Statistical Computing. Retrieved from https://www.R-project.org/

Ramos-López, D., Masegosa, A. R., Salmerón, A., Rumí, R., Langseth, H., Nielsen, T. D., & Madsen, A. L. (2018). Scalable importance sampling estimation of Gaussian mixture posteriors in Bayesian networks. *International Journal of Approximate Reasoning*, *100*, 115–134. https://doi.org/10.1016/j.ijar.2018.06.004

Ruggiero, P., Kaminsky, G. M., Gelfenbaum, G., & Cohn, N. (2016). Morphodynamics of prograding beaches: A synthesis of seasonal- to century-scale observations of the Columbia River littoral cell. *Marine Geology*, *376*, 51–68. https://doi.org/10.1016/j.margeo.2016.03.012

Ruggiero, P., Kaminsky, G. M., Gelfenbaum, G., & Voigt, B. (2005). Seasonal to interannual morphodynamics along a high-energy dissipative littoral cell. *Journal of Coastal Research*, *213*(3), 553–578. https://doi.org/10.2112/03-0029.1

Ruggiero, P., Kratzmann, M. A., Himmelstoss, E. G., Reid, E., Allan, J. C., & Kaminsky, G. M. (2013). National assessment of shoreline change: Historical shoreline change along the Pacific Northwest Coast (Open-File Report 2012-1007 No. U.S. Geological Survey Open-File Report 2012-1007) (p. 62). US Geological Survey. Retrieved from https://doi.org/10.3133/ofr20121007

Sallenger, A. H. (2000). Storm impact scale for barrier islands. *Journal of Coastal Research*, *16*(3), 890–895.

Salmerón, A., Rumí, R., Langseth, H., Madsen, A. L., & Nielsen, T. D. (2015). MPE inference in conditional linear Gaussian networks. In S. Destercke, & T. Denoeux (Eds.), *Symbolic and quantitative approaches to reasoning with uncertainty*, (pp. 407–416). Springer International Publishing. https://doi.org/10.1007/978-3-319-20807-737

Saye, S. E., van der Wal, D., Pye, K., & Blott, S. J. (2005). Beach–dune morphological relationships and erosion/accretion: An investigation at five sites in England and Wales using LIDAR data. *Geomorphology*, *72*(1–4), 128–155. https://doi.org/10.1016/j.geomorph.2005.05.007

Scutari, M., & Denis, J.-B. (2014). *Bayesian networks with examples in R*. Boca Raton: Chapman and Hall. https://doi.org/10.1201/b17065

Seabloom, E. W., & Wiedemann, A. M. (1994). Distribution and effects of *Ammophila breviligulata* Fern. (American beachgrass) on the foredunes of the Washington coast. *Journal of Coastal Research*, *10*(1), 178–188.

Short, A. D., & Hesp, P. A. (1982). Wave, beach and dune interactions in southeastern Australia. *Marine Geology*, *48*(3-4), 259–284. https://doi.org/10.1016/0025-3227(82)90100-1

Spalding, M. D., Ruffo, S., Lacambra, C., Meliane, I., Hale, L. Z., Shepard, C. C., & Beck, M. W. (2014). The role of ecosystems in coastal protection: Adapting to climate change and coastal hazards. *Ocean & Coastal Management*, *90*, 50–57. https://doi.org/10.1016/j.ocecoaman.2013.09.007

Stockdon, H. F., Sallenger, A. H., Holman, R. A., & Howd, P. A. (2007). A simple model for the spatially-variable coastal response to hurricanes. *Marine Geology*, *238*(1-4), 1–20. https://doi.org/10.1016/j.margeo.2006.11.004

Sutton-Grier, A. E., Wowk, K., & Bamford, H. (2015). Future of our coasts: The potential for natural and hybrid infrastructure to enhance the resilience of our coastal communities, economies and ecosystems. *Environmental Science & Policy*, *51*, 137–148. https://doi.org/10.1016/j.envsci.2015.04.006

Trifonova, N., Kenny, A., Maxwell, D., Duplisea, D., Fernandes, J., & Tucker, A. (2015). Spatio-temporal Bayesian network models with latent variables for revealing trophic dynamics and functional networks in fisheries ecology. *Ecological Informatics*, *30*, 142–158. https://doi.org/10.1016/j.ecoinf.2015.10.003

Van Dijk, P., Arens, S., & Van Boxel, J. (1999). Aeolian processes across transverse dunes. II: Modelling the sediment transport and profile development. *Earth Surface Processes and Landforms*, *24*(4), 319–333. https://doi.org/10.1002/(SICI)1096-9837(199904)24:4<319::AID-ESP963>3.0.CO;2-M

Walker, I. J., Davidson-Arnott, R. G., Bauer, B. O., Hesp, P. A., Delgado-Fernandez, I., Ollerhead, J., & Smyth, T. A. (2017). Scale-dependent perspectives on the geomorphology and evolution of beach-dune systems. *Earth-Science Reviews*, *171*, 220–253. https://doi.org/10.1016/j.earscirev.2017.04.011

Wiedemann, A. M. (1984). The ecology of Pacific Northwest coastal sand dunes: A community profile (No. FWS/OBS-84/04). Washington, D.C.: U.S. Fish and Wildlife Service.

Wiedemann, A. M., & Pickart, A. (1996). The *Ammophila* problem on the Northwest coast of North America. *Landscape and Urban Planning*, *34*(3–4), 287–299. https://doi.org/10.1016/0169-2046(95)00240-5

Wright, L. D., & Short, A. D. (1984). Morphodynamic variability of surf zones and beaches: A synthesis. *Marine Geology*, *56*(1–4), 93–118. https://doi.org/10.1016/0025-3227(84)90008-2

Zarnetske, P. L., Hacker, S. D., Seabloom, E. W., Ruggiero, P., Killian, J. R., Maddux, T. B., & Cox, D. (2012). Biophysical feedback mediates effects of invasive grasses on coastal dune shape. *Ecology*, *93*(6), 1439–1450. https://doi.org/10.1890/11-1112.1

Zarnetske, P. L., Ruggiero, P., Seabloom, E. W., & Hacker, S. D. (2015). Coastal foredune evolution: the relative influence of vegetation and sand supply in the US Pacific Northwest. *Journal of The Royal Society Interface*, *12*(106). https://doi.org/10.1098/rsif.2015.0017